Nonlinear Dynamics **15:** 311–327, 1998.

Resonances of a Harmonically Forced Duffing Oscillator with Time Delay State Feedback

HAIYAN HU
Institute of Vibration Engineering Research, Nanjing University of Aeronautics and Astronautics, 210016 Nanjing, P.R. China

EARL H. DOWELL and LAWRENCE N. VIRGIN
Department of Mechanical Engineering and Material Sciences, School of Engineering, Duke University, Durham, NC 27708, U.S.A.

(Received: 5 February 1997; accepted: 6 October 1997)

Abstract. The paper presents analytical and numerical studies of the primary resonance and the 1/3 subharmonic resonance of a harmonically forced Duffing oscillator under state feedback control with a time delay. By using the method of multiple scales, the first order approximations of the resonances are derived and the effect of time delay on the resonances is analyzed. The concept of an equivalent damping related to the delay feedback is proposed and the appropriate choice of the feedback gains and the time delay is discussed from the viewpoint of vibration control. In order to numerically solve the problem of history dependence prior to the start of excitation, the concepts of the Poincaré section and fixed points are generalized. Then, a modified shooting scheme associated with the path following technique is proposed to locate the periodic motion of the delayed system. The numerical results show the efficacy of the first order approximations of the resonances.

Keywords: Time delay, stability, vibration control, periodic motion.

1. Introduction

The last decade has witnessed an increasing number of studies and applications of the active control of mechanical and structural vibrations in various fields. Superior as the active control is over the passive control in many aspects, it involves more technical problems. One of the open problems is the complicated system dynamics induced by the unavoidable time delays in controllers and actuators, especially in various analogue filters, hydraulic and pneumatic actuators, where the time delays may give rise to the instability of the controlled systems.

Great attention has been paid to the stability analysis of delay controlled systems over the past decades [1, 2], but mainly in the context of linear dynamic systems. The work on nonlinear dynamic systems under delay control so far has focused on the dynamics of systems described by autonomous difference-differential equations. For instance, the Hopf bifurcation of a system equilibrium has been intensively studied in recent mathematical publications [3, 4] and dealt with in various engineering fields [5–7]. To the authors' knowledge, the dynamics of the delayed non-autonomous systems, e.g., periodically forced nonlinear systems under delay control, have received less attention [8].

The objective of this paper is to analyze the dynamics of a non-autonomous delayed system. As the first study, a harmonically forced Duffing oscillator under linear time delay control is considered. This system serves as the simplest model for various controlled nonlinear

systems, e.g., active vehicle suspension systems when the nonlinearity in tires is taken into account [5]. The system motion is described by a second order nonlinear difference-differential equation

$$m\frac{\mathrm{d}^2x(\bar{t})}{\mathrm{d}\bar{t}^2}+c\frac{\mathrm{d}x(\bar{t})}{\mathrm{d}\bar{t}}+kx(\bar{t})+\mu kx^3(\bar{t})=\bar{u}x(\bar{t}-\bar{\tau})+\bar{v}\frac{\mathrm{d}x(\bar{t}-\bar{\tau})}{\mathrm{d}\bar{t}}+F\cos\omega\bar{t}, \tag{1}$$

where $m>0$, $k>0$ and $0<\bar{\tau}\le 2\pi/\omega$. By using the following dimensionless time and new parameters

$$\begin{cases} t=\sqrt{\dfrac{k}{m}}\,\bar{t}, \quad \tau=\sqrt{\dfrac{k}{m}}\,\bar{\tau}\,, \quad u=\dfrac{\bar{u}}{2k}\,, \quad v=\dfrac{\bar{v}}{2\sqrt{mk}}\,, \\ \zeta=\dfrac{c}{2\sqrt{mk}}\,, \ f=\dfrac{F}{k}\,, \quad \lambda=\omega\sqrt{\dfrac{m}{k}}\,, \end{cases} \tag{2}$$

Equation (1) can be written as

$$\frac{\mathrm{d}^2x}{\mathrm{d}t^2}(t)+2\zeta\frac{\mathrm{d}x}{\mathrm{d}t}(t)+x(t)+\mu x^3(t)=2ux(t-\tau)+2v\frac{\mathrm{d}x}{\mathrm{d}t}(t-\tau)+f\cos\lambda t. \tag{3}$$

In the following two sections, the primary and the 1/3 subharmonic resonances will be respectively studied by using the method of multiple scales. Presented in Section 4 are the concepts and associated numerical technique for locating the periodic motions of the delay controlled systems, which are by nature infinite dimensional. The comparisons between the analytical and numerical results are given in Section 5.

2. Primary Resonance

2.1. Steady-State Resonance

To analyze the primary resonance of the delay controlled system (3) by using the method of multiple scales, we confine the study to the case of small damping, weak nonlinearity, weak feedback and soft excitation. That is,

$$\begin{cases} \zeta=O(\varepsilon), \ \ \mu=O(\varepsilon), \quad u=O(\varepsilon), \ \ v=O(\varepsilon), \\ f=O(\varepsilon), \ \ \lambda-1=\varepsilon\sigma, \ \ \sigma=O(1), \end{cases} \tag{4}$$

where $0<\varepsilon\ll 1$ and σ is the detuning frequency. Rewrite Equation (3) as

$$\begin{aligned} \frac{\mathrm{d}^2x}{\mathrm{d}t^2}(t)+x(t) \ = \ & -2\zeta\frac{\mathrm{d}x}{\mathrm{d}t}(t)-\mu x^3(t)+2ux(t-\tau) \\ & +2v\frac{\mathrm{d}x}{\mathrm{d}t}(t-\tau)+f\cos(1+\varepsilon\sigma)t. \end{aligned} \tag{5}$$

For simplicity, we assume a two scale expansion of the solution

$$x(t)=x_0(T_0,T_1)+\varepsilon x_1(T_0,T_1)+O(\varepsilon^2), \quad T_r=\varepsilon^r t, \quad r=0,1, \tag{6}$$

and use the following differential operators [9]

$$\begin{cases} \dfrac{\mathrm{d}}{\mathrm{d}t} = \dfrac{\partial}{\partial T_0} + \varepsilon \dfrac{\partial}{\partial T_1} + O(\varepsilon^2) \equiv D_0 + \varepsilon D_1 + O(\varepsilon^2), \\ \dfrac{\mathrm{d}^2}{\mathrm{d}t^2} = D_0^2 + 2\varepsilon D_0 D_1 + O(\varepsilon^2). \end{cases} \tag{7}$$

Substituting Equations (6) and (7) into Equation (5) and equating the same power of ε, we obtain a set of linear partial differential equations

$$D_0^2 x_0(T_0, T_1) + x_0(T_0, T_1) = 0, \tag{8a}$$

$$\begin{aligned} D_0^2 x_1(T_0, T_1) + x_1(T_0, T_1) = & -2D_0 D_1 x_0(T_0, T_1) - 2\zeta D_0 x_0(T_0, T_1) - \mu x_0^3(T_0, T_1) \\ & + 2u x_0(T_0 - \tau, T_1) + 2v D_0 x_0(T_0 - \tau, T_1) + f \cos(T_0 + \sigma T_1). \end{aligned} \tag{8b}$$

Solving Equation (8a) for $x_0(T_0, T_1)$, we have

$$x_0(T_0, T_1) = A(T_1) e^{iT_0} + \mathrm{cc}, \tag{9}$$

where 'cc' denotes the conjugate term and

$$A(T_1) \equiv \frac{1}{2} \alpha(T_1) e^{i\beta(T_1)}. \tag{10}$$

Substituting Equation (9) into Equation (8b) yields

$$\begin{aligned} D_0^2 x_1(T_0, T_1) + x_1(T_0, T_1) \; = \; & -2i D_1 A e^{iT_0} - 2i\zeta A e^{iT_0} - \mu(A^3 e^{3iT_0} + 3A^2 \bar{A} e^{iT_0}) \\ & + 2u e^{-i\tau} A e^{iT_0} + 2iv e^{-i\tau} A e^{iT_0} + \frac{f}{2} e^{i\sigma T_1} e^{iT_0} + \mathrm{cc}. \end{aligned} \tag{11}$$

To eliminate the secular term in Equation (11), we let

$$-2i(D_1 + \zeta - v e^{-i\tau}) A + 2u A e^{-i\tau} - 3\mu A^2 \bar{A} + \frac{f}{2} e^{i\sigma T_1} = 0. \tag{12}$$

By substituting Equation (10) into Equation (12) and separating the real part and the imaginary part, we obtain a set of autonomous differential equations that govern the amplitude $\alpha(T_1)$ and the phase $\varphi(T_1)$

$$\begin{cases} D_1 \alpha = -(\zeta + u \sin\tau - v \cos\tau)\alpha + \dfrac{f}{2} \sin\varphi, \\ \alpha D_1 \varphi = (\sigma + u \cos\tau + v \sin\tau)\alpha - \dfrac{3\mu}{8} \alpha^3 + \dfrac{f}{2} \cos\varphi, \end{cases} \tag{13}$$

where

$$\varphi(T_1) = \sigma T_1 - \beta(T_1). \tag{14}$$

From Equation (13), we have a set of algebraic equations for amplitude $\hat{\alpha}$ and phase $\hat{\varphi}$ of the steady-state primary resonance

$$\begin{cases} -(\zeta + u\sin\tau - v\cos\tau)\hat{\alpha} + \dfrac{f}{2}\sin\hat{\varphi} = 0, \\ (\sigma + u\cos\tau + v\sin\tau)\hat{\alpha} - \dfrac{3\mu}{8}\hat{\alpha}^3 + \dfrac{f}{2}\cos\hat{\varphi} = 0, \end{cases} \tag{15}$$

whereby we derive the frequency response relation between $\hat{\alpha}$ and σ, and that between $\hat{\varphi}$ and σ

$$\begin{cases} [(\zeta + u\sin\tau - v\cos\tau)^2 + (\sigma + u\cos\tau + v\sin\tau - \dfrac{3\mu}{8}\hat{\alpha}^2)^2]\hat{\alpha}^2 - \dfrac{f^2}{4} = 0, \\ \tan\hat{\varphi} + \dfrac{\zeta + u\sin\tau - v\cos\tau}{\sigma + u\cos\tau + v\sin\tau - (3\mu/8)\hat{\alpha}^2} = 0. \end{cases} \tag{16}$$

Given a specific value of $\hat{\alpha}$, one can readily solve the first equation in Equation (16) for σ, and then obtain $\hat{\varphi}$ from the second equation. Hence, one has the first order approximation of the steady-state primary resonance

$$x(t) = \hat{\alpha}\cos(\lambda t - \hat{\varphi}) + O(\varepsilon). \tag{17}$$

Figure 1 shows the amplitude and phase of the primary resonance *versus* the excitation frequency for the uncontrolled system, the controlled system without time delay, and the controlled system with different time delays.

2.2. Stability Analysis

To analyze the stability of the steady-state primary resonance, we linearize Equation (13) at $(\hat{\alpha}, \hat{\varphi})$ with respect to α and φ

$$\begin{cases} D_1\Delta\alpha = -(\zeta + u\sin\tau - v\cos\tau)\Delta\alpha + \dfrac{f}{2}\cos\hat{\varphi}\Delta\varphi, \\ D_1\Delta\varphi = -\left(\dfrac{3\mu}{4}\hat{\alpha}^2 + \dfrac{f}{2\hat{\alpha}^2}\cos\hat{\varphi}\right)\Delta\alpha - \dfrac{f}{2\hat{\alpha}}\sin\hat{\varphi}\Delta\varphi. \end{cases} \tag{18}$$

The characteristic equation of Equation (18), thus, is

$$\det\begin{bmatrix} -(\zeta + u\sin\tau - v\cos\tau) - s & \dfrac{f}{2}\cos\hat{\varphi} \\ -\left(\dfrac{3\mu}{4}\hat{\alpha}^2 + \dfrac{f}{2\hat{\alpha}^2}\cos\hat{\varphi}\right) & -\dfrac{f}{2\hat{\alpha}}\sin\hat{\varphi} - s \end{bmatrix} = 0. \tag{19}$$

According to Equation (15), Equation (19) can be simplified to

$$s^2 + 2as + b = 0, \tag{20}$$

where

$$\begin{cases} a = \zeta + u\sin\tau - v\cos\tau, \\ b = \left(\dfrac{a}{2}\right)^2 + \left(\sigma + u\cos\tau + v\sin\tau - \dfrac{3\mu}{8}\hat{\alpha}^2\right)\left(\sigma + u\cos\tau + v\sin\tau - \dfrac{9\mu}{8}\hat{\alpha}^2\right). \end{cases} \tag{21}$$

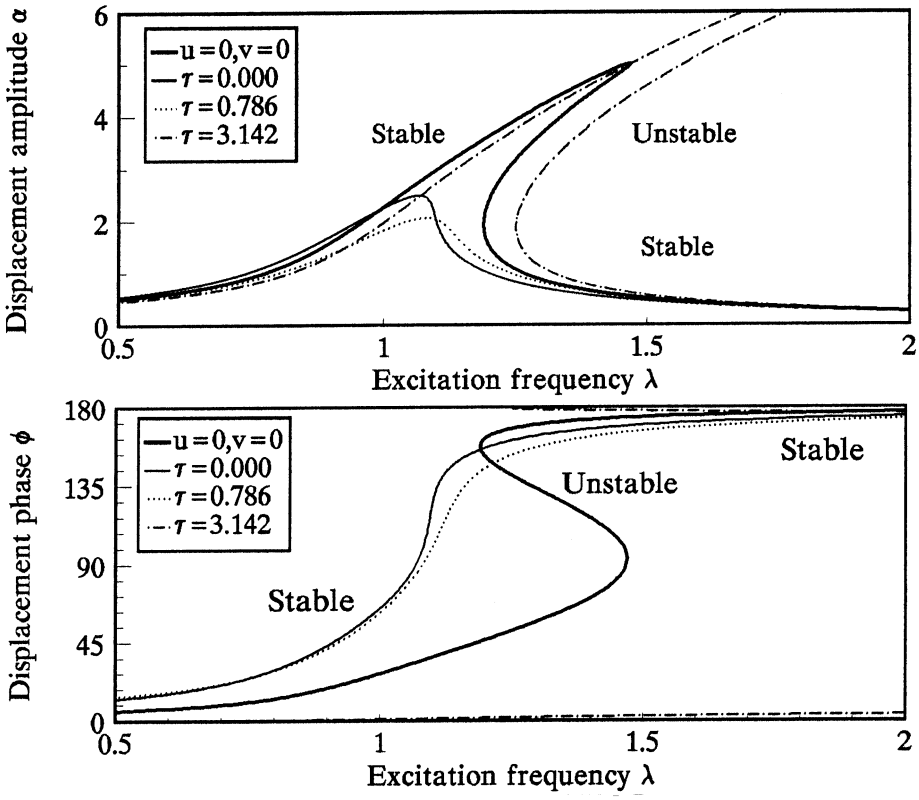

Figure 1. Frequency-amplitude and frequency-phase relations of the primary resonance ($\zeta = 0.05$, $\mu = 0.05$, $f = 0.5$, $u = 0$, $v = 0$, or $u = 0.05$, $v = -0.05$).

From the Routh–Hurwitz criterion, the steady-state vibration is asymptotically stable if and only if the following two inequalities hold simultaneously

$$\begin{cases} a = \zeta + u\sin\tau - v\cos\tau > 0, \\ b = \left(\dfrac{a}{2}\right)^2 + \left(\sigma + u\cos\tau + v\sin\tau - \dfrac{3\mu}{8}\,\hat{\alpha}^2\right)\left(\sigma + u\cos\tau + v\sin\tau - \dfrac{9\mu}{8}\,\hat{\alpha}^2\right) > 0. \end{cases} \tag{22}$$

The first condition in Equation (22) is independent of the nonlinearity, the resonance amplitude, and hence the excitation. As a matter of fact, it serves as the stability condition for the free vibration of the linear system with delay feedback. Letting

$$\frac{\mathrm{d}a}{\mathrm{d}\tau} \equiv u\cos\tau + v\sin\tau = 0, \tag{23}$$

one can obtain an infinite number of time delays

$$\tau_r = \tan^{-1}\left(-\frac{u}{v}\right) + r\pi, \quad r = 0, 1, 2, \ldots \tag{24}$$

at which a goes to the extreme values

$$a_{\min} = \zeta - \sqrt{u^2 + v^2}, \quad a_{\max} = \zeta + \sqrt{u^2 + v^2}. \tag{25}$$

This implies that if the feedback gains are so small that $\sqrt{u^2+v^2} < \zeta$, the stability of the free vibration of the linear system is independent of the time delay in the state feedback.

By calculating the condition $\mathrm{d}\sigma/\mathrm{d}\hat{\alpha} = 0$, one can readily find that the critical case of $b = 0$ corresponds to the two turning points on the curve of σ–$\hat{\alpha}$. Thus, the stability of the primary resonance of the Duffing oscillator with delay feedback is qualitatively the same as that of the delay-free Duffing oscillator. When the time delay yields Equation (23), the second condition in Equation (22) becomes

$$b = \left(\zeta \pm \sqrt{u^2+v^2}\right)^2 + \left(\sigma - \frac{3\mu}{8}\,\hat{\alpha}^2\right)\left(\sigma - \frac{9\mu}{8}\,\hat{\alpha}^2\right) > 0. \tag{26}$$

2.3. Amplitude Peak

Substituting Equation (25) into the first equation in Equation (16), one obtains

$$\left[\left(\zeta \pm \sqrt{u^2+v^2}\right)^2 + \left(\sigma - \frac{3\mu}{8}\,\hat{\alpha}^2\right)^2\right]\hat{\alpha}^2 - \frac{f^2}{4} = 0. \tag{27}$$

Hence, the amplitude peak of the primary resonance yields

$$\hat{\alpha}_{\max} = \frac{f}{2(\zeta \pm \sqrt{u^2+v^2})}\,. \tag{28}$$

This implies that if the time delay is appropriately chosen so that $a = a_{\max} = \zeta + \sqrt{u^2+v^2}$, the amplitude peak can be reduced to a minimum by the state feedback. On the other hand, the state feedback will greatly increase the amplitude peak if the time delay makes $a = a_{\min} = \zeta - \sqrt{u^2+v^2}$. This property enables one to design an appropriate time delay in the feedback in order to enhance the control performance.

2.4. Equivalent Damping Ratio

It is interesting that the quantity a defined in Equation (21) takes the role of the damping ratio in the standard forced Duffing oscillator. That is, it governs not only the stability of the resonance, but also the amplitude peak of the primary resonance. For simplicity, a will be referred to as the equivalent damping ratio of the delay controlled system. In Figure 1, the equivalent damping ratios at the time delay $\tau = 0.786 \approx \pi/4$ and $\tau = 3.142 \approx \pi$ are $a \approx a_{\max} \approx 0.1207$ and $a \approx 0$, respectively. The corresponding peaks of the displacement amplitude reach the minimum and infinity, respectively. Furthermore, when a happens to vanish, the system response will include the free vibration that does not decay. This may result in a quasiperiodic motion if the frequency ratio of the free vibration and the forced vibration is not a rational number. Anyhow, this case should be avoided from the viewpoint of vibration control, for the critically stable response is very dangerous.

Now we consider the negative velocity feedback ($v < 0$), which has been widely used to reduce steady-state vibration in engineering. In this case, Equation (24) gives $\tau_r = r\pi$ since $u = 0$. The optimal control performance, hence, can be realized only when there is no time delay or there is a long time delay, say, $\tau = 2\pi$ in the velocity feedback. If displacement feedback is introduced, we have the following linear approximation of Equation (21) for short time delay

$$a \approx \zeta + |v| + u\tau + o(\tau). \tag{29}$$

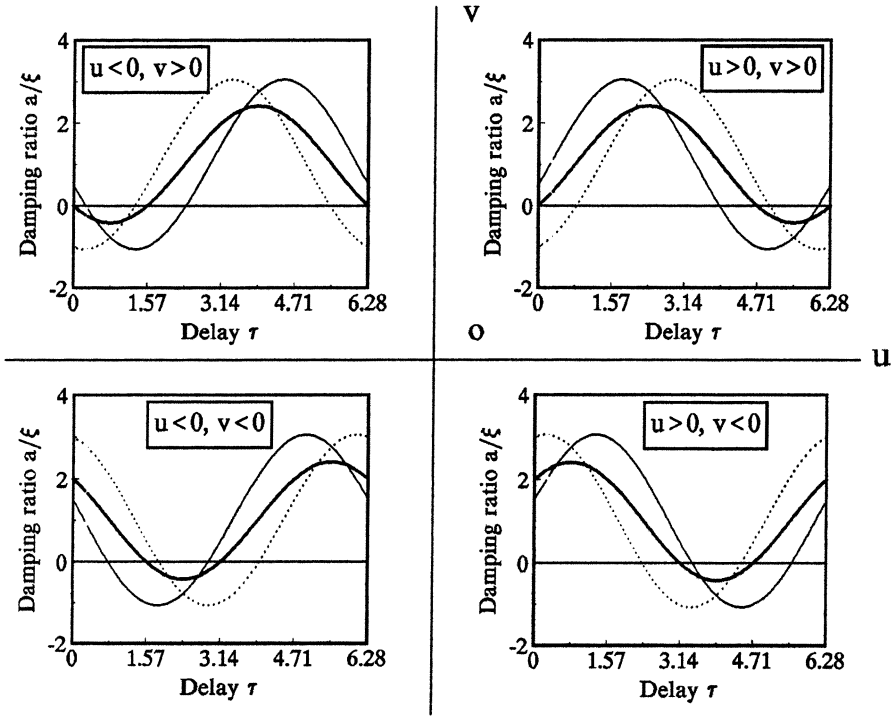

Figure 2. Relations between ratio a/ζ and delay τ at various feedback gains u and v (thick curves: $|u| = |v| = 1.0$, thin curves: $|u| = 2.0$, $|v| = 0.5$, dotted curves: $|u| = 0.5$, $|v| = 2.0$).

This implies that the control performance can be better than the optimal one of the velocity feedback only, if the displacement feedback gain u is positive.

Figure 2 shows the variation of ratio a/ζ with increase in time delay τ under different combinations of the feedback gains. One can readily see from Figure 2 that the equivalent damping ratio is optimal when the feedback gains yield $u > 0$ and $v < 0$, because it decreases to zero at the longest time delay. This shows again that the positive displacement feedback will improve the vibration control performance of the negative velocity feedback.

3. 1/3 Subharmonic Resonance

3.1. Steady-State Resonance

To study the 1/3 subharmonic resonance of the controlled system, we confine ourselves to the case of

$$\zeta = O(\varepsilon), \quad \mu = O(\varepsilon), \quad u = O(\varepsilon), \quad v = O(\varepsilon), \quad \lambda - 3 = \varepsilon\sigma, \quad \sigma = O(1), \tag{30}$$

but release the excitation from the small magnitude. Rewrite Equation (3) as

$$\begin{aligned} \frac{\mathrm{d}^2x}{\mathrm{d}t^2}(t) + x(t) &= -2\zeta\frac{\mathrm{d}x}{\mathrm{d}t}(t) - \mu x^3(t) + 2ux(t-\tau) \\ &\quad + 2v\frac{\mathrm{d}x}{\mathrm{d}t}(t-\tau) + f\cos(3+\varepsilon\sigma)t. \end{aligned} \tag{31}$$

Substituting Equations (6) and (7) into Equation (31) and equating the same power of ε, we obtain

$$D_0^2 x_0(T_0, T_1) + x_0(T_0, T_1) = f\cos(3T_0 + \sigma T_1), \tag{32a}$$

$$\begin{aligned} D_0^2 x_1(T_0, T_1) + x_1(T_0, T_1) \;=\; & -2D_0 D_1 x_0(T_0, T_1) - 2\zeta D_0 x_0(T_0, T_1) - \mu x_0^3(T_0, T_1) \\ & + 2u x_0(T_0 - \tau, T_1) + 2v D_0 x_0(T_0 - \tau, T_1). \end{aligned} \tag{32b}$$

By solving Equation (32a) for $x_0(T_0, T_1)$, we have

$$x_0(T_0, T_1) = A(T_1)e^{iT_0} + Ge^{i(3T_0+\sigma T_1)} + \text{cc}, \quad G = \frac{f}{2(1-\lambda^2)}. \tag{33}$$

Substituting Equation (33) into Equation (32b) yields

$$\begin{aligned} & D_0^2 x_1(T_0, T_1) + x_1(T_0, T_1) \\ & \quad = (-2iD_1 A - 2i\zeta A - 6\mu A G^2 - 3\mu A^2 \bar{A} + 2ue^{-i\tau} A + 2ive^{-i\tau} A)e^{iT_0} \\ & \qquad - 3\mu \bar{A}^2 G e^{i(T_0+\sigma T_1)} + \cdots. \end{aligned} \tag{34}$$

The secular term of Equation (34) vanishes if and only if

$$2i(D_1 A + \zeta A - ve^{-i\tau} A) - 2ue^{-i\tau} A + 6\mu A G^2 + 3\mu A^2 \bar{A} + 3\mu \bar{A}^2 G e^{i\sigma T_1} = 0. \tag{35}$$

Substituting Equation (10) into Equation (35) and separating the real part and the imaginary part, we obtain the autonomous differential equations governing the amplitude and the phase

$$\begin{cases} D_1\alpha = -(\zeta + u\sin\tau - v\cos\tau)\alpha - \dfrac{3\mu G\alpha^2}{4}\sin\phi, \\ \\ D_1\phi = (\sigma + 3u\cos\tau + 3v\sin\tau - 9\mu G^2) - \dfrac{9\mu}{8}\alpha^2 - \dfrac{9\mu G\alpha}{4}\cos\phi, \end{cases} \tag{36}$$

where

$$\phi(T_1) = \sigma T_1 - 3\beta(T_1). \tag{37}$$

From Equation (36), we get a set of algebraic equations that governs the amplitude $\hat{\alpha}$ and the phase $\hat{\phi}$ of the steady-state 1/3 subharmonic resonance

$$\begin{cases} (\zeta + u\sin\tau - v\cos\tau)\hat{\alpha} = -\dfrac{3\mu G\hat{\alpha}^2}{4}\sin\hat{\phi}, \\ \\ (\sigma + 3u\cos\tau + 3v\sin\tau - 9\mu G^2) - \dfrac{9\mu}{8}\hat{\alpha}^2 = \dfrac{9\mu G\hat{\alpha}}{4}\cos\hat{\phi}, \end{cases} \tag{38}$$

whereby we have the frequency response relation between $\hat{\alpha}$ and σ and that between $\hat{\phi}$ and σ

$$\begin{cases} 9(\zeta + u\sin\tau - v\cos\tau)^2 \\ \qquad + \left(\sigma + 3u\cos\tau + 3v\sin\tau - 9\mu G^2 - \dfrac{9\mu}{8}\hat{\alpha}^2\right)^2 - \left(\dfrac{9\mu G\hat{\alpha}}{4}\right)^2 = 0, \\ \\ \tan\hat{\phi} + \dfrac{3(\zeta + u\sin\tau - v\cos\tau)}{\sigma + 3u\cos\tau + 3v\sin\tau - 9\mu G^2 - (9\mu/8)\hat{\alpha}^2} = 0. \end{cases} \tag{39}$$

The first order approximation for the steady-state 1/3 subharmonic resonance reads

$$x(t) = \hat{\alpha} \cos\left(\frac{\lambda t - \hat{\phi}}{3}\right) + \frac{f}{1-\lambda^2} \cos \lambda t. \tag{40}$$

One can expand the first equation in Equation (39) as

$$\hat{\alpha}^4 - 2P\hat{\alpha}^2 + Q = 0, \tag{41}$$

and solve it for $\hat{\alpha}$

$$\hat{\alpha} = \sqrt{P \pm \sqrt{P^2 - Q}}\,, \tag{42}$$

where

$$\begin{cases} P = \dfrac{8}{9\mu}\,(\sigma + 3u\cos\tau + 3v\sin\tau) - 6G^2, \\ \\ Q = \dfrac{64}{81\mu^2}\,[9(\zeta + u\sin\tau - v\cos\tau)^2 + (\sigma + 3u\cos\tau + 3v\sin\tau - 9\mu G^2)^2]. \end{cases} \tag{43}$$

Equation (42) requires $P > 0$ and $P^2 > Q$ since $Q > 0$. Substituting Equation (43) into these inequalities, one obtains

$$\begin{cases} \dfrac{27\mu}{4}\,G^2 < (\sigma + 3u\cos\tau + 3v\sin\tau), \\ \\ \left|\dfrac{63\mu}{4}\,G^2 - (\sigma + 3u\cos\tau + 3v\sin\tau)\right| \\ \quad \le \sqrt{(\sigma + 3u\cos\tau + 3v\sin\tau)^2 - 63(\zeta + u\sin\tau - v\cos\tau)^2}. \end{cases} \tag{44}$$

It is easy to prove that the second inequality covers the first, and hence gives the existence condition of the 1/3 subharmonic resonance. This condition can be readily converted into one with respect to the dimensionless excitation amplitude f and excitation frequency λ.

Figure 3 shows the existence regions of the 1/3 subharmonic resonance in the plane of f and λ for the uncontrolled system, the controlled system without time delay, and those with time delays corresponding to $a \approx a_{\max}$ and $a \approx 0$, respectively. Figure 4 gives the amplitude and phase of the 1/3 subharmonic resonance *versus* the excitation frequency for these systems subject to the same level of excitation. Obviously, the equivalent damping ratio governs the threshold of the excitation amplitude and frequency for the occurrence of the 1/3 subharmonic resonance, so does the time delay. However, it is not so effective to reduce the amplitude of the 1/3 subharmonic resonance as in the control of primary resonance by choosing a proper time delay.

3.2. Stability Analysis

To analyze the stability of the steady-state subharmonic resonance, we linearize Equation (36) at $(\hat{\alpha}, \hat{\phi})$ with respect to α and ϕ

$$\begin{cases} D_1\Delta\alpha = -\left(\zeta + u\sin\tau - v\cos\tau + \dfrac{3\mu G\hat{\alpha}}{2}\sin\hat{\phi}\right)\Delta\alpha - \dfrac{3\mu G\hat{\alpha}^2}{4}\cos\hat{\phi}\Delta\phi, \\ \\ D_1\Delta\phi = -\dfrac{9\mu}{4}\,(\hat{\alpha} + G\cos\hat{\phi})\Delta\alpha + \dfrac{9\mu G\hat{\alpha}}{4}\sin\hat{\phi}\Delta\phi. \end{cases} \tag{45}$$

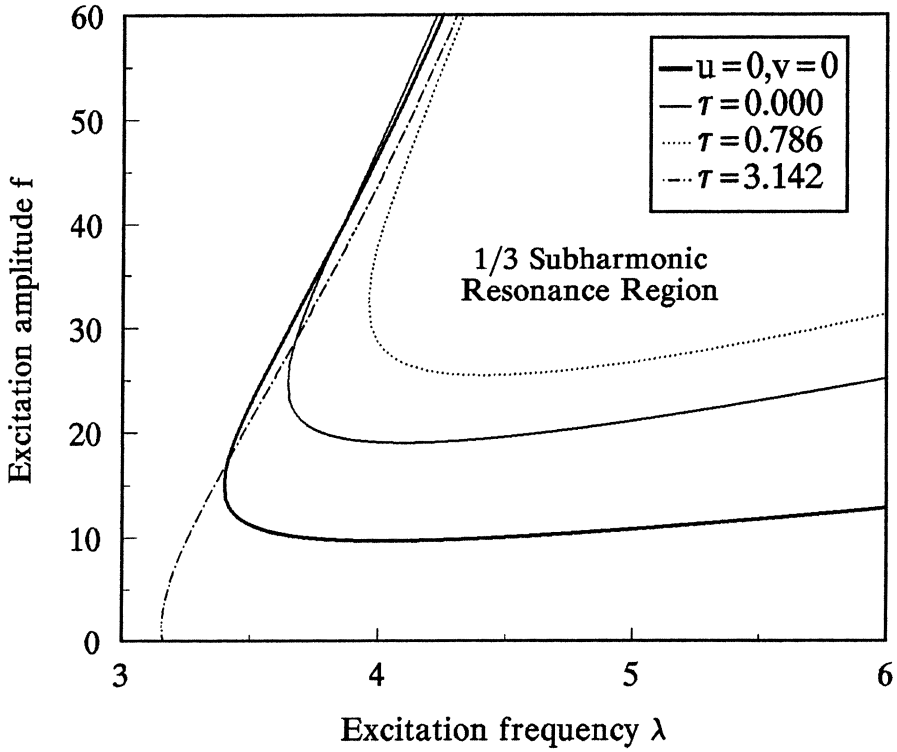

Figure 3. Threshold of the excitation amplitude and frequency at different time delays ($\zeta = 0.05$, $\mu = 0.05$, $u = 0$, $v = 0$, or $u = 0.05$, $v = -0.05$).

The characteristic equation of Equation (45) has the form

$$\det \begin{bmatrix} -\left(\zeta + u\sin\tau - v\cos\tau + \dfrac{3\mu G\hat{\alpha}}{2}\sin\hat{\phi}\right) - s & -\dfrac{3\mu G\hat{\alpha}^2}{4}\cos\hat{\phi} \\ -\dfrac{9\mu}{4}(\hat{\alpha} + G\cos\hat{\phi}) & -\dfrac{9\mu G\hat{\alpha}}{4}\sin\hat{\phi} - s \end{bmatrix} = 0. \tag{46}$$

By using Equation (38) and the first equation in Equation (43), the characteristic equation can be simplified to

$$s^2 + 2as + d = 0, \tag{47}$$

where

$$\begin{cases} a = \zeta + u\sin\tau - v\cos\tau, \\ d = -\dfrac{27\mu^2\hat{\alpha}^2}{32}(P - \hat{\alpha}^2). \end{cases} \tag{48}$$

The 1/3 subharmonic resonance is asymptotically stable if and only if

$$a > 0, \quad \hat{\alpha}^2 > P. \tag{49}$$

The first inequality here shows that the equivalent damping ratio takes an important role again in the stability of the subharmonic resonance. The second inequality implies that the

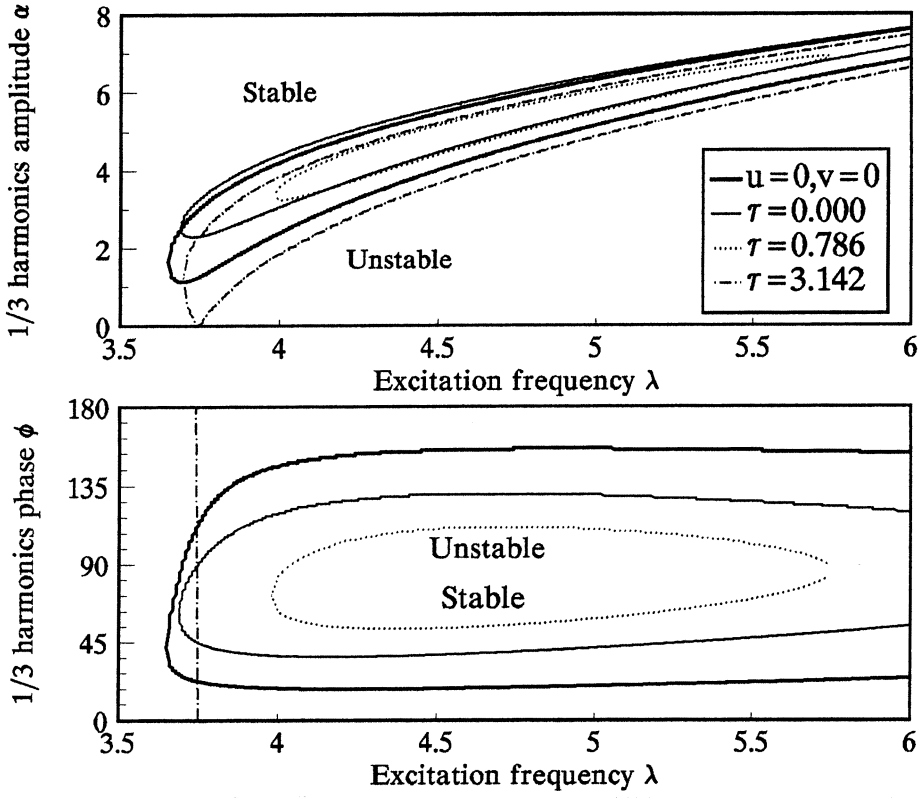

Figure 4. Frequency-amplitude and frequency-phase relations of 1/3 subharmonic resonance ($\zeta = 0.05$, $\mu = 0.05$, $f = 30$, $u = 0$, $v = 0$, or $u = 0.05$, $v = -0.05$).

upper branch solution in Equation (41) is asymptotically stable as shown in Figure 4, while the lower branch solution is not.

4. Shooting Scheme for Locating Periodic Motions

In this section, we study how to compute the periodic solutions of difference-differential equation (3) numerically so as to verify the approximate results in Sections 2 and 3. As shown in those two sections, there exist more than one periodic motion and one of them is unstable if the primary resonance or 1/3 subharmonic resonance occurs. Thus, the shooting technique, rather than the direct numerical integration, will be discussed in order to determine the co-existing periodic motions, including the unstable one.

4.1. Basic Concepts

We first write the initial value problem of Equation (3) as a set of first order non-autonomous difference-differential equations in the two-dimensional state space spanned by $\mathbf{y} \equiv [x, \dot{x}]^T$

$$\begin{cases} \dfrac{\mathrm{d}\mathbf{y}(t)}{\mathrm{d}t} = \mathbf{f}(\mathbf{y}(t), \mathbf{y}(t-\tau), t, \lambda), & t \geq 0, \\ \mathbf{y}(t) = \mathbf{y}_0(t), & t \in [-\tau, 0], \quad 0 < \tau \leq T = 2\pi/\lambda; \end{cases} \tag{50}$$

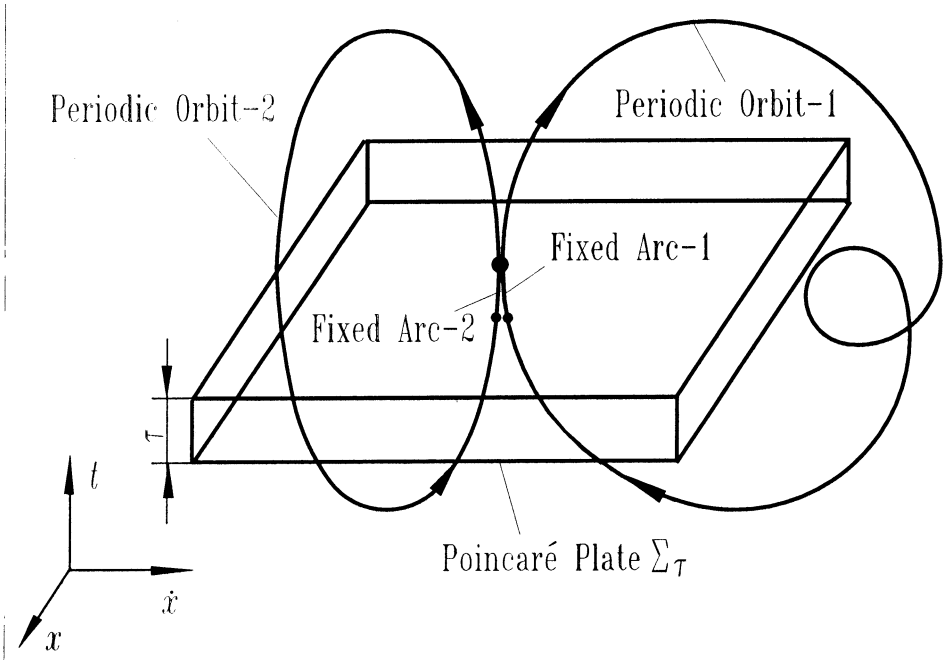

Figure 5. Generalization of the Poincaré section and the fixed point for locating the periodic orbit of a delayed system.

where

$$\mathbf{f}(\mathbf{y}(t), \mathbf{y}(t-\tau), t, \lambda) = \begin{bmatrix} \dot{x}(t) \\ -x(t) - \mu x^3(t) - 2\zeta\dot{x}(t) + 2ux(t-\tau) + 2\dot{v}(t-\tau) + f\cos\lambda t \end{bmatrix}, \tag{51}$$

$$\mathbf{y}_0(t) \equiv [x_0(t), \dot{x}_0(t)]^T. \tag{52}$$

An important feature of this set of difference-differential equations is that the initial condition should be a given function $x_0(t)$ in the time interval $[-\tau, 0]$, rather than a single initial state at the instant of $t = 0$. The solution space of Equation (50), therefore, is infinite dimensional. However, $\dot{x}_0(t)$ is not an independent initial condition.

Now, we consider the Poincaré mapping, which conceptually simplifies the task of finding a periodic orbit of the differential equation to locating the corresponding fixed point $\mathbf{y}_F$. However, if one defines the Poincaré section Σ_0 to be a fixed excitation phase ψ and establishes the corresponding Poincaré mapping $\mathbf{P}_0 : \Sigma_0 \to \Sigma_0$, one cannot determine the unique periodic orbit Γ of Equation (50) from the fixed point $\mathbf{y}_F$ of the Poincaré mapping $\mathbf{P}_0$. This is because there exist an infinite number of trajectories that start from $\mathbf{y}_F$, whereas the periodic orbit Γ should be the one that coincides with the piece of itself in the previous phase interval $[\psi - \tau, \psi]$, not only at the fix point $\mathbf{y}_F$.

To establish the one-to-one correspondence between the Poincaré mapping and Equation (50), the Poincaré section can intuitively be generalized to the 'Poincaré Plate' Σ_τ with the thickness of τ, as shown in Figure 5. The corresponding Poincaré mapping $\mathbf{P}_\tau : \Sigma_\tau \to \Sigma_\tau$ maps a scalar function $x(t)$ to the function $\mathbf{P}_\tau(x(t))$ over the interval $[\psi - \tau, \psi]$, and hence becomes an infinite dimensional mapping. The original fixed point $\mathbf{y}_P$ should be generalized

to a 'Fixed Arc' $x_F(t)$ under the infinite dimensional Poincaré mapping. It is the segment of the periodic orbit Γ intersecting with the Poincaré plate.

4.2. Shooting Scheme

The task of shooting a periodic orbit of Equation (50) is to locate the fixed arc $x_F(t)$, $t \in [\psi - \tau, \psi]$. A straightforward extension of the current shooting scheme is to approximate the candidate arc $x(t)$, $t \in [\psi - \tau, \psi]$ in shooting by using $N - 1$ line segments and shoot the N nodes of these segments. No doubt that the longer the dimensionless time delay τ in control, the more line segments must be used in the shooting procedure.

Specifically, let $\mathbf{z} = [x_1, x_2, \ldots, x_N]^T$ denote the vector of node co-ordinates on the candidate arc $x(t)$, $t \in [\psi - \tau, \psi]$, where

$$x_i = x(t_i), \quad t_i = -\tau + (i-1)\tau/(N-1), \quad i = 1, 2, \ldots, N. \tag{53}$$

The shooting procedure based on the Newton–Raphson iteration is as below

$$\mathbf{z}_{k+1} = \mathbf{z}_k - [\mathbf{DP}(\mathbf{z}_k) - \mathbf{I}]^{-1}[\mathbf{P}(\mathbf{z}_k) - \mathbf{z}_k], \quad k = 0, 1, 2, \ldots, \tag{54}$$

where $\mathbf{P} : \mathbf{z} \to \mathbf{z}$ is the N-dimensional approximate mapping for $\mathbf{P}_\tau$ and $\mathbf{DP}$ is its Jacobian. In the following, we present how to compute $\mathbf{P}(\mathbf{z}_k)$ and $\mathbf{DP}(\mathbf{z}_k)$ in Equation (54). For the sake of simplicity, the subscript of $\mathbf{z}_k$ will be omitted.

The mapping $\mathbf{P}(\mathbf{z})$ can be computed by integrating Equation (50) as follows. At first, one can calculate $\dot{\mathbf{z}} = [\dot{x}_1, \dot{x}_2, \ldots, \dot{x}_N]^T$ from $\mathbf{z} = [x_1, x_2, \ldots, x_N]^T$ by using numerical differentiation and obtain the discrete values of $\mathbf{y}_0(t)$, $t \in [-\tau, 0]$. Then, one simply needs to integrate the following differential equations

$$\frac{\mathrm{d}\mathbf{y}_{j+1}(t)}{\mathrm{d}t} = \mathbf{f}(\mathbf{y}_{j+1}(t), \mathbf{y}_j(t-\tau), t, \lambda), \quad t \in [(j-1)\tau, j\tau], \quad j = 0, 1, 2, \ldots \tag{55}$$

successively until $t \geq T$ through the use of available codes, say, the Runge–Kutta scheme. If the ratio T/τ is an integer, one happens to obtain

$$\mathbf{P}(\mathbf{z}) = [x(t_1 + T), x(t_2 + T), \ldots, x(t_N + T)]^T. \tag{56}$$

Otherwise, it is necessary to interpolate every $x(t_i + T)$ in Equation (56) from its two neighbor values.

The Jacobian $\mathbf{DP}$ is the solution matrix $\mathbf{Z}(T)$ of the initial value problem of the following set of linear difference-differential equations

$$\begin{cases} \dfrac{\mathrm{d}}{\mathrm{d}t}\mathbf{Z}(t) = \mathbf{D}_1\mathbf{f}(\mathbf{z}(t), \mathbf{z}(t-\tau), t, \lambda)\mathbf{Z}(t) \\ \qquad\qquad + \mathbf{D}_2\mathbf{f}(\mathbf{z}(t), \mathbf{z}(t-\tau), t, \lambda)\mathbf{Z}(t-\tau), \qquad t > 0, \\ \mathbf{Z}(t) = \underset{1 \leq i \leq N}{\mathrm{diag}}\,\{\delta(t - t_i)\}, \qquad\qquad t \in [-\tau, 0]; \end{cases} \tag{57}$$

where

$$\mathbf{z}(t) \equiv [x(t_1 + t), x(t_2 + t), \ldots, x(t_N + t)]^T, \tag{58}$$

$$\delta(t) \equiv \begin{cases} 1, & t = 0, \\ 0, & t \neq 0, \end{cases} \tag{59}$$

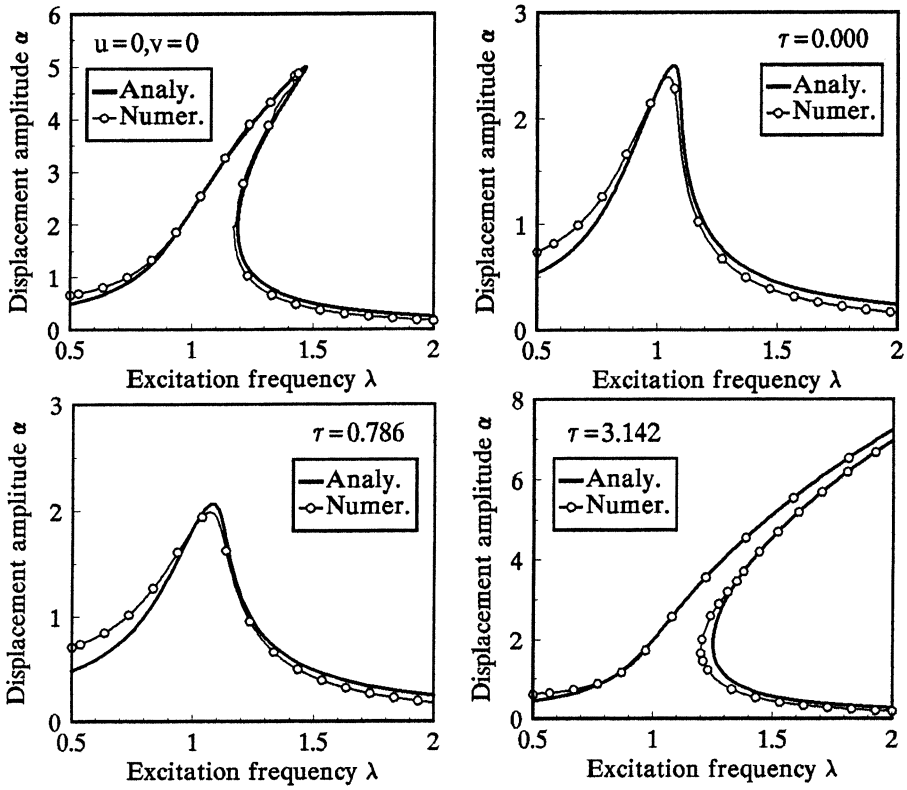

Figure 6. Primary resonance amplitudes computed by multiple scale method and shooting method ($\zeta = 0.05$, $\mu = 0.05$, $f = 0.5$, $u = 0$, $v = 0$, or $u = 0.05$, $v = -0.05$).

$\mathbf{D}_1$ and $\mathbf{D}_2$ are the derivative operators with respect to $\mathbf{z}(t)$ and $\mathbf{z}(t-\tau)$, respectively. To obtain the Jacobian **DP**, Equation (57) should be simultaneously integrated with Equation (50) by using the codes for computing $\mathbf{P}(\mathbf{z})$.

The shooting procedure can be incorporated with the parametric continuation technique to determine the unknown periodic orbits of the nonlinear delay system from a known periodic orbit of the simplified systems. For instance, one can start from the periodic orbit of the delay-free system and take the time delay τ as the continuation parameter.

5. Comparisons between Analytical and Numerical Results

5.1. Primary Resonance

Figure 6 shows the primary resonance amplitudes *versus* the excitation frequency obtained by the method of multiple scales in Section 2 and the shooting scheme in Section 4 for four typical parametric combinations as in Figure 1. Here, the results of the shooting scheme can be considered as the exact resonance amplitudes including the higher order terms of $O(\varepsilon)$ neglected in Section 2. It is obvious that the approximate analytical results coincide with the exact results very well, except in the lower frequency range when the equivalent damping ratio is large. The comparison supports the assertion that the properly selected time delay increases the equivalent damping ratio so that the primary resonance can be attenuated effectively.

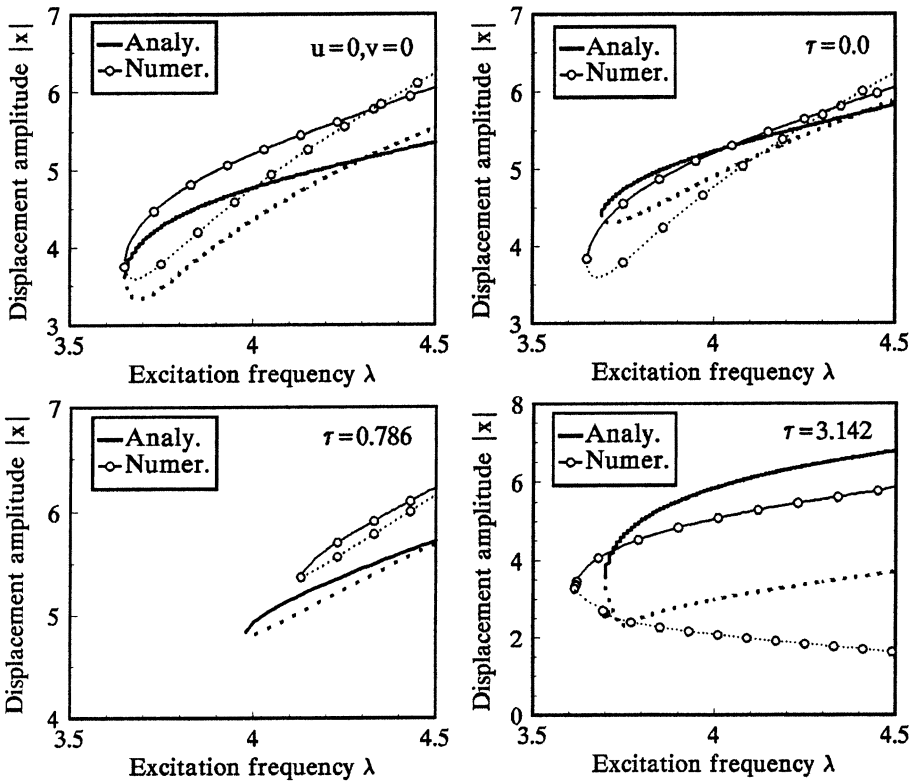

Figure 7. 1/3 subharmonic resonance amplitudes computed by multiple scale method and shooting method ($\zeta = 0.05$, $\mu = 0.05$, $f = 30$, $u = 0$, $v = 0$, or $u = 0.05$, $v = -0.05$).

5.2. 1/3 Subharmonic Resonance

In Figure 7 are shown the amplitudes of the 1/3 subharmonic resonance *versus* the excitation frequency obtained by the two methods for four typical parametric combinations, where the dotted curves indicate the unstable resonances. It should be noted that the amplitude here is the maximal value of the displacement, instead of the amplitude of 1/3 harmonic component only. Of course, the self-intersections of the amplitude curves only mean the amplitudes of the stable motion and the unstable motion are the same at a specific excitation frequency, rather than any bifurcations, because the phases of these two motions are totally different.

Compared with the primary resonance, the subharmonic resonances given by the method of multiple scales deviate substantially from the exact results, but are acceptable for some engineering applications. As shown in Figure 8, the subharmonic and harmonic amplitudes obtained by the two methods are almost the same, while the phase difference between the results causes the above mentioned deviation. The numerical result in the case of $\tau = 0.786$ supports again the important role taken by the proper time delay in avoiding the occurrence of the 1/3 subharmonic resonance.

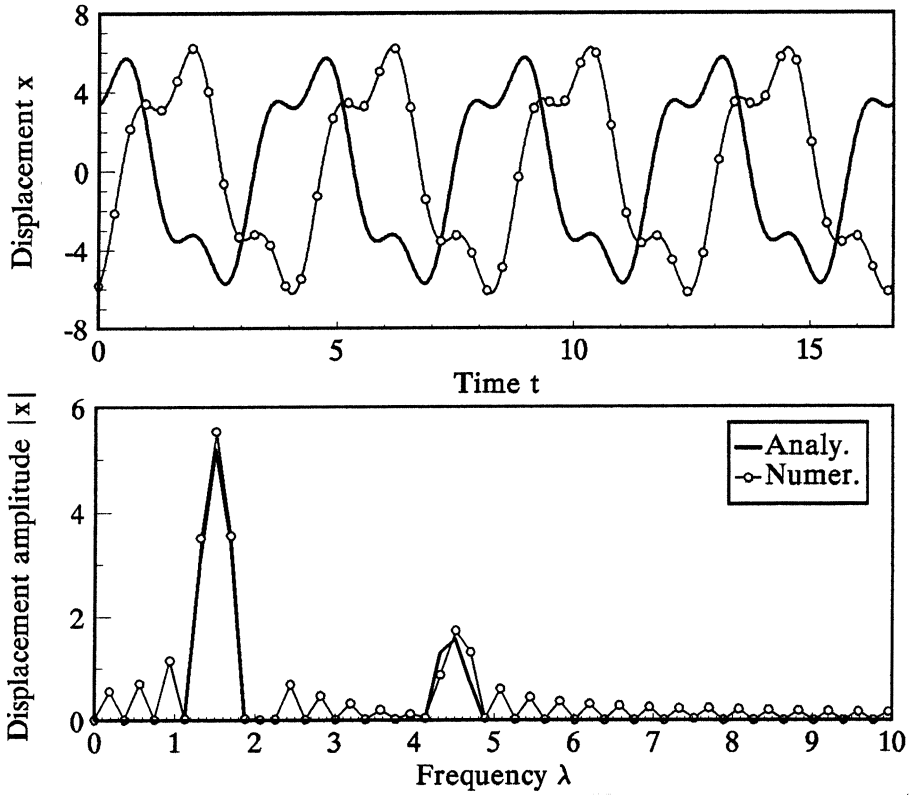

Figure 8. Time histories and Fourier spectrums of 1/3 subharmonic resonance computed by multiple scale method and shooting method ($\zeta = 0.05$, $\mu = 0.05$, $f = 30$, $\lambda = 4.5$, $u = 0.05$, $v = -0.05$).

6. Concluding Remarks

The time delay in the feedback control results in an infinite dimension for the controlled nonlinear system, and increases dramatically the complexity of the numerical analysis for the system dynamics. The method of multiple scales proves to be a powerful tool to gain insight into the primary resonance and subharmonic resonance of the Duffing oscillator with weak nonlinearity and weak delay feedback. It can similarly be used to analyze the superharmonic resonance and combined resonance of this oscillator. Furthermore, the method of multiple scales is applicable to other weakly nonlinear systems, e.g., the active suspension system involving the weakly quadratic nonlinearity in tires, as long as the gains of delay feedback are small enough.

The primary resonance and the 1/3 subharmonic resonance of the harmonically forced Duffing oscillator with delay state feedback are qualitatively the same as those of the uncontrolled Duffing oscillator subject to harmonic excitation when the dimensionless feedback gains are the same order as the small linear damping ratio. From the viewpoint of vibration control, however, the time delay takes an important role in providing active damping, which governs the resonance stability and the amplitude peak. The combination of positive displacement feedback and negative velocity feedback is the most advantageous one for attenuating those resonances. Furthermore, a proper choice of time delay can enhance the control performance.

Acknowledgments

This work was supported in part by the National Funds for Outstanding Young Scientists of China under grant No. 59625511 and in part by the International Research Scholarship of China.

References

1. Hale, J., *Theory of Functional Differential Equations*, Springer-Verlag, New York, 1977.
2. Gopalsamy, K., *Stability and Oscillations in Delay Differential Equations of Population Dynamics*, Kluwer, Dordrecht, 1992.
3. Diekmann, O., van Gils, S. A., Verduyn Lunel, S. M., and Walther, H.-O., *Delay Equations, Functional, Complex, and Nonlinear Analysis*, Springer-Verlag, New York, 1995.
4. Belair, J. and Campbell, S. A., 'Stability and bifurcation of equilibria in a multi-delayed differential equation', *SIAM Journal on Applied Mathematics* **54**(5), 1994, 1402–1424.
5. Palkovics, L. and Venhovens, P. J. Th., 'Investigation on stability and possible chaotic motions in the controlled wheel suspension system', *Vehicle System Dynamics* **21**(5), 1992, 269–296.
6. Stepan, G. and Haller, G., 'Quasiperiodic oscillations in robot dynamics', *Nonlinear Dynamics* **8**(4), 1995, 513–528.
7. Moiola, J. L., Chiacchiarini, H. G., and Desages, A. C., 'Bifurcations and Hopf degeneracies in nonlinear feedback systems with time delay', *International Journal of Bifurcation and Chaos* **6**(4), 1996, 661–672.
8. Plaut, R. H. and Hsieh, J. C., 'Non-linear structural vibrations involving a time delay in damping', *Journal of Sound and Vibration* **117**(3), 1987, 497–510.
9. Nayfeh, A. H. and Mook, D. T., *Nonlinear Oscillations*, Wiley, New York, 1979.